MATEC Web of Conferences **165**, 22007 (2018) https://doi.org/10.1051/matecconf/201816522007
FATIGUE 2018

Identification of fatigue damage evolution in 316L stainless steel using acoustic emission and digital image correlation

Farhan Tanvir[1,2*], *Tariq* Sattar[1], *David* Mba[3], *Graham* Edwards[4], *Elvin* Eren[4], and *Yoann* Lage[5]

[1]London South Bank University, 103 Borough Rd, London SE1 0AA, UK
[2]NSIRC, TWI Ltd, Granta Park, Great Abington, Cambridge, CB21 6AL, UK
[3]De Montfort University, Gateway House, Leicester LE1 9BH, UK
[4] TWI Ltd, Granta Park, Great Abington, Cambridge, CB21 6AL, UK
[5]Mistras Group Ltd, Norman Way, Over, Cambridge CB24 5QE, UK

Abstract. One of the main objectives of Acoustic Emission (AE) monitoring is to identify approaching critical stage of damage in the structure before it fails. State-of-the-art AE analysis is done on the features in both the time and frequency domains. Many features such as centroid frequency, duration, rise-time, count and energy are dependent on acquisition settings; threshold and timing parameters. Incorrect acquisition settings may result in inaccurate classification of the AE source. This work proposes a new feature in the time domain signal based on 2nd order Renyi's entropy, which proves to be efficient in identifying different stages of damage. Renyi's entropy is a measure of uncertainty or randomness of the signals and is directly derived from the distribution of signal amplitude. Therefore, it is independent of threshold and timing parameters. The validity of the proposed parameter is investigated by performing AE monitoring during fatigue endurance test of 316L stainless steel. Digital Image Correlation (DIC) and global strain monitoring was carried out to relate material damage with AE activity. The result shows Renyi's entropy to be an effective measure to identify critical stages of damage in the material.

1. Introduction

Fatigue damage has been a matter of interest for years. It is expected that almost half of mechanical failure is due to fatigue. In Liquid Natural Gas (LNG) containment, sloshing is the dominant fatigue damage mechanism that causes structural failure. Therefore, for safety and reliability, it is important to monitor fatigue damage in these structures.

Acoustic Emission (AE) [1], is capable of identifying different stages of damage in the material and has shown potential as a Structural Health Monitoring (SHM) method [2] [3]. In comparison with other Non-Destructive Test (NDT) methods, AE can provide location and characterization of the damage in real time. AE monitoring utilizes sensors and data acquisition equipment to detect the elastic waves generated in the material as a result of damage. AE signals can be measured using several parameters including rise-time, duration, energy, count, peak amplitude, etc. Figure 1 below highlights the definitions of these parameters.

AE has been shown to be sensitive to different stages in damage growth. There are several sources of damage that contribute to AE, including plastic yielding, micro facture, crack initiation, crack propagation and crack rubbing [4]. The crack initiation has been shown to be accompanied by a significant increase in the peak amplitude, cumulative count and energy of the AE [5]. Han et al. [6] [7], suggested AE features such as count rate, peak amplitude and rise-time are sensitive to three different stages of fatigue; stage 1 fatigue crack initiation, stage 2 slow fatigue crack propagation and stage 3 rapid crack propagation. Han et al. [7] [8] distinguished other cracking mechanisms based on peak amplitude and rise time observation such as twinning, crack extension, cleavage facture, plastic zone activity, ligament shearing between micro-voids and micro-cracks. The change in facture mode from tensile to shear has been shown to be accompanied by a sharp increase in the duration and rise time of the signal [9]. Robert et al. [10], demonstrated the prediction of crack length based on the count rate of the signal.

Most of the studies conducted above are based on parametric analysis of AE signals. Except for peak amplitude, AE parameters (explained in fig 1) are, dependent on acquisition settings such as threshold and timing. Different settings will result in different AE calculated parameters.

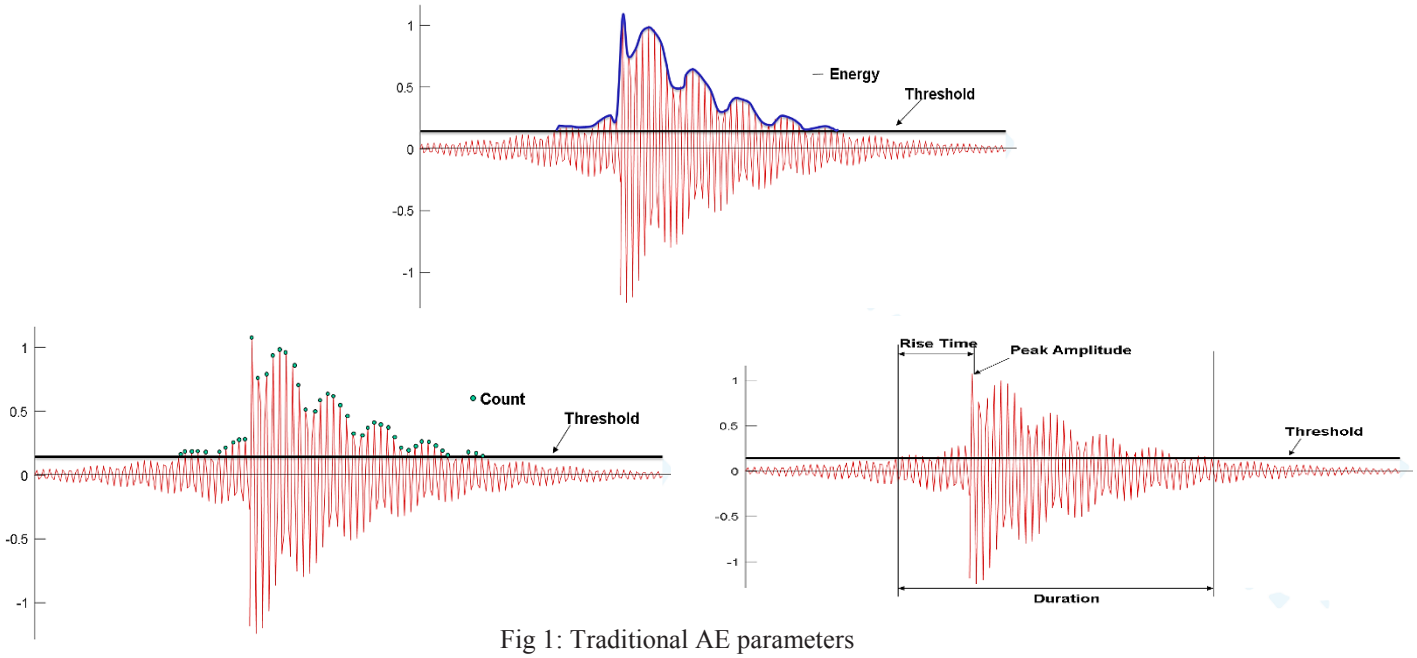

Fig 1: Traditional AE parameters

Recently, entropy of a signal in the time domain has been shown to be independent of acquisition settings. This is because it is derived from the probability mass in the amplitude distribution of signals and has shown to be effective in AE monitoring during fatigue [11] [12]. However, the work performed in [11] [12] is on the basis of Shannon's entropy, which is based on a linear averaging operator. The entropy computation in this research is based on second order Renyi's entropy. Renyi's entropy is based on the second functional class called the non-linear averaging operator, which has been proved to be more flexible and accurate than Shannon's entropy. Renyi's entropy computed in this work is compared with traditional AE parameters and has proved to be equally effective in discriminating damage in the material. Entropy of a signal is a measure of disorder and randomness in the signal. It is shown in this work that signals from material damage are associated with a higher value of entropy (higher randomness and disordered) than that of noise.

2. Methodology

2.1. Experimental Procedure

Dog-bone sample of 316L stainless steel, designed according to the standard E466-15 was used for the test (figure 2). Tables 1 and 2 show the chemical composition and mechanical properties of the specimen respectively. Fatigue endurance tests on the specimen was carried out with an Instron servo-hydraulic testing machine at ambient temperature. The specimen was tested under sinusoidal cyclic loading, with constant frequency of 5Hz, peak load of 24KN and loading ratio of 0.1.

AE signals from the fatigue test were recorded and analysed by an AMSY-6 data acquisition system controlled by Vallen software. Two AE sensors with a peak sensitivity frequencies between 100 kHz to 450 kHz and preamplifiers with a gain of 34dB were used. The distance between the sensors for the test was 90mm. Hit Definition Time (HDT) of 400µs, Re-Arm-Time of 1ms and threshold of 40dB were used as the data acquisition settings. Duration based Transient Recording (TR) was used for the test with a maximum TR page length of 26,214µs. A 1D location processor for 1D linear source localization was used with a wave velocity calibration of 5000m/s. The localisation facilitates the elimination of the noise generated from metal to metal contact at the grip, by recording signals generated only from the gauge section of the specimen.

In order to relate material response with AE activity, the specimen was monitored simultaneously with other NDT techniques. Two tests were conducted in total. The first test was conducted with simultaneous AE and global strain measurement. The second test was conducted with simultaneous AE, global strain and Digital Image Correlation (DIC) measurement. In order to perform DIC measurement, blocks of pixels were introduced in the gauge section of the specimen on the side of the specimen opposite the AE sensors. An ARAMIS-5m DIC system with a frame rate of 15Hz up to 29Hz and camera resolution of 2448 x 2050 px was used to capture the 2D displacement field of the pixel blocks. The frequency of the images taken by the DIC system was 0.005Hz.

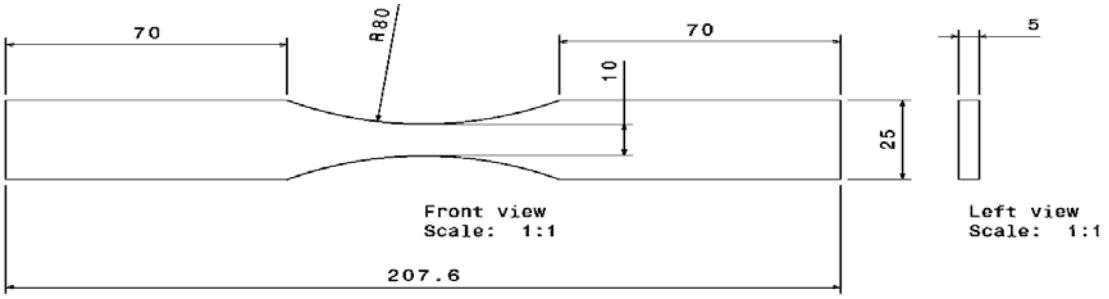

Fig 2: Dog-bone fatigue endurance specimen

Table1: Chemical Composition

C	Mn	P	S	Si	Cu	Ni	Cr	Mo	Nb
0.025	1.32	0.03	0.002	0.48	0.36	10.03	16.58	2.02	0.041

Table2: Mechanical Properties

Young's Modulus	193GPA
Yield Strength (Longitudinal) **Rp** 1%	347MPA
Tensile Strength (Longitudinal)	613MPA

2.2. Renyi's Entropy

In the 1950s, Alfred Renyi introduced a parametric family of information theory called Renyi's entropy that generalizes Shannon's entropy [13]. Renyi pointed out that Shannon's entropy estimation is based on the first functional class which is the linear averaging operator($g(x) = cx$). He proposed an entropy formulation based on the second functional class called the non-linear averaging operator ($g(x) = c2^{(1-a)x}$) which proved to be more flexible than that of Shannon's formulation [14].

Entropy is based on the measure of uncertainty in a probability distribution function and is widely used in mathematics and physics [15]. Given a random sequence$\{x_1 x_2 x_3, \ldots., x_n\}$, Renyi's entropy is calculated according to equation (1), as:

$$\mathrm{H_a}(x) = \frac{1}{1-\mathrm{a}} \log\left(\sum_{k=1}^{\mathrm{n}} (P(x_k))^{\mathrm{a}}\right) \quad (1)$$

Where:-

$H_a(x)$ is Renyi's entropy

$P(x_k)$ is the probability mass associated with the value x_1.

a is the order of the equation, which is selected to be 2 in this paper.

Log to the base 2 is used in this case in order to measure the entropy in bits. Log to the base 10 or $\log_e$ can also be used in order to measure entropy in bins and bans respectively. For simplicity, Renyi's entropy will be referred to as AE entropy in this paper. The fundamental reason for using AE entropy is its independency from acquisition settings such as threshold and timing, unlike traditional AE parameters. The calculation procedure of AE entropy begins with recording AE waveform generated from the experiment using the AE monitoring system. The waveform captured from the experiment is converted into a txt file containing millivolt and microsecond values. The discrete probability distribution of the waveform is then calculated. Several methods have been proposed to calculate the probability of mass in order to calculate the entropy of a digital waveform [16] [17]. The probability of mass calculation in this work is based on taking into account the original spectrum of the signal, explained in [16]. Probability of mass for entropy calculation, by taking into account the original spectrum of the signal has been widely used in signal processing [18] [19]. After probability of mass calculation, AE entropy is calculated using eqn 1. Figure 3 below shows the AE entropy calculation steps.

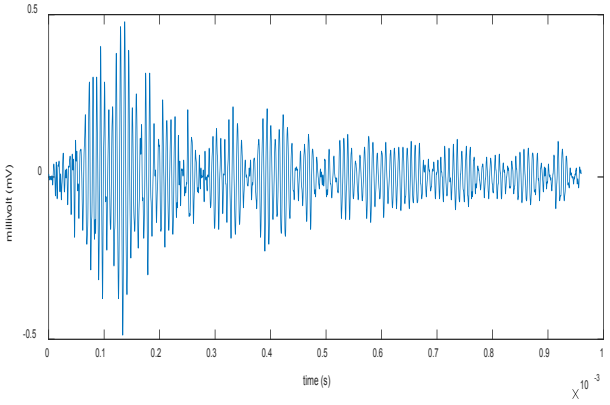

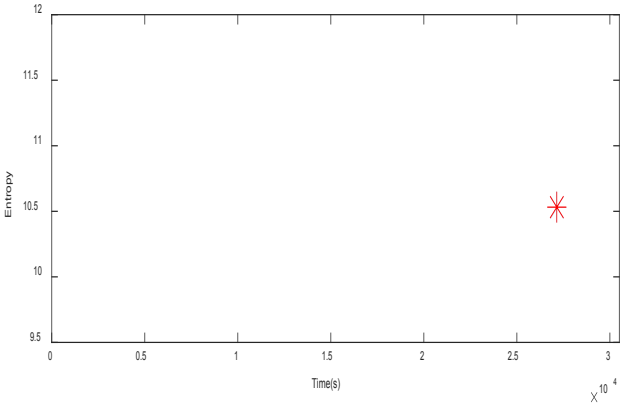

x_1	0.009134
x_2	0.003045
x_3	0.003045
.....	.....
x_{4799}	0.015223
x_{4800}	0.012178
x_{4801}	0.009134

X=x		P(X=x)
0	0.009134	0.0016
1	0.003045	0.0002
2	0.003045	0.0002
…	….	….
4799	0.015223	0.0045
4800	0.012178	0.0029
4801	0.009134	0.0016

Fig 3: Entropy calculation steps

3. Results and Discussions

3.1. AE data collection with %elongation of the specimen

A plot of peak amplitude of the AE waveform and % elongation of the specimen versus time was recorded during the cyclic loading of the test machine (figure 4).

The initial part of the test is accompanied by a significant increase in the peak amplitude (up to 92dB) of the signal and % elongation of the specimen. At this stage of the test, signals in the lower amplitude range are associated with elastic to plastic transformation of the material [20] [21], whereas signals in the higher amplitude range (above 60dB) could originate from initial metal to metal contact noise [22]. Subsequently, signals with lower amplitude (below 55dB) start to appear up to about 14,000s. The time from the onset of loading until 14,000s can be regarded as the damage accumulation or crack nucleation stage.

It can be observed in figure 5, a plot of count rate and %elongation versus time that up to 14,000s, except for the onset of loading, there is a low count rate, suggesting that at this stage there is damage accumulation or crack nucleation [23] [24]. The initial increase in count rate at the onset of loading is due to the enhanced micro-structural activity due to elastic to plastic transformation and noise due to loading train. At the end of this stage the damage becomes localized, micro cracks start to appear and join to form the short cracks [24]. Figure 5 also shows a sudden increase in count rate of the signals after 14,000s. The increase in count rate here is associated with micro damage of the material such as growth and coalescence of micro crack [24]. By comparing with figure 4, an increase in count rate is also accompanied by high amplitude signals at 14,000s and 18,000s (above 55dB) as a result of the micro damage in the material.

After 25,000s the damage becomes visibly localized and both count rate and peak amplitude increase significantly, due to macro fatigue crack initiation, growth and ultimate failure. Peak amplitude of the signal is a useful parameter for identifying damage mechanisms in a material. However, it is difficult in this experiment to accurately identify damage mechanism such as growth and coalescence of micro crack based on peak amplitude observation alone, as it is possible to confuse the initial jump in peak amplitude, at the onset of loading, to be from the material damage.

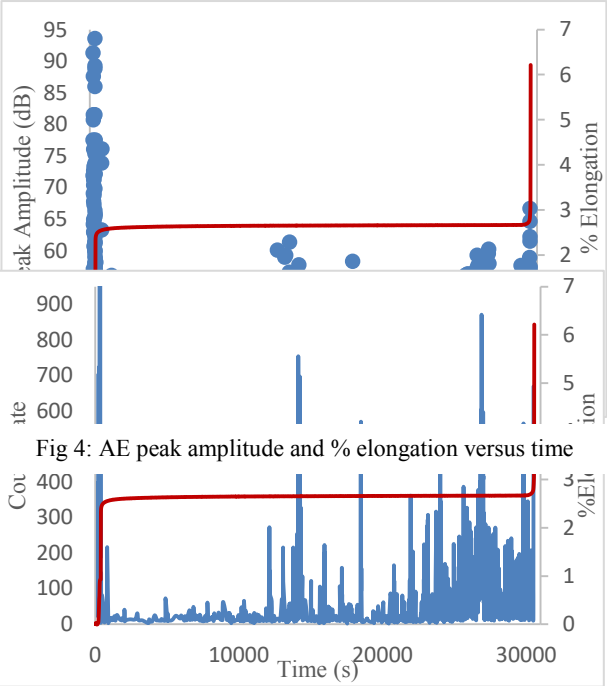

Fig 4: AE peak amplitude and % elongation versus time

Fig 5: AE Count Rate rate and % elongation versus time

As an alternative to peak amplitude parameter, a threshold independent parameter called AE entropy was calculated from the recorded waveforms, as explained in section 1. The plot of AE entropy and % elongation versus time is shown in figure 6.

It is evident from figure 6 that waveform with higher peak amplitude in the beginning of the test is associated with a lower value of AE entropy (below 11). During the damage accumulation stage, up to 14,000s, entropy variation turned out to be stable. The waveform captured at 14,000s showed a sudden rise in AE entropy, higher than that at the beginning, which was caused by elastic to plastic transformation and mechanical noise. The sudden rise in AE entropy after 14,000s is also accompanied by a sudden rise in count rate of the signal, observed in figure 5, suggesting these signals to be originating from enhanced micro-structural activity, such as growth and coalescence of micro crack [23] [24].

Waveforms captured at 18,000s also showed an increase in AE entropy accompanied by a sharp increase in the count rate. However, the increase in AE entropy at 18,000s is not very significant as compared to the AE entropy at 14,000s. This could be due to a small magnitude of micro damage as compared to the one at 14,000s.

AE Entropy was stable until 23,000s. At approximately 25,000s damage in the specimen was visibly localized and was accompanied by a significant increase in both the count rate and AE entropy of the signal leading to the macro fatigue crack initiation, growth and ultimate failure of the specimen. A significant number of signals after 25,000s, were associated with AE entropy that was higher than the entropy at the onset of cyclic loading.

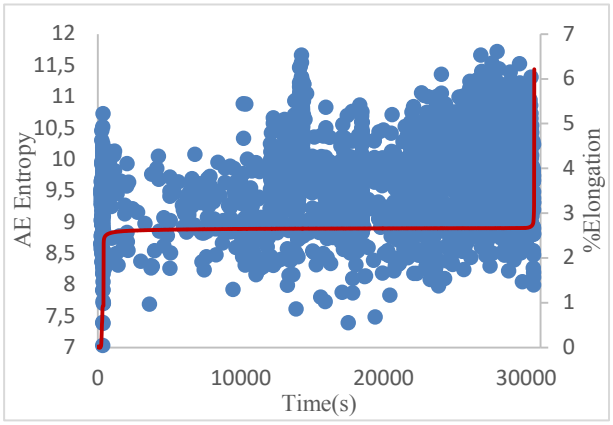

Fig 6: AE entropy and % elongation versus time

Figure 7 illustrates a comparison of cumulative count, cumulative energy and cumulative entropy for the entire length of the test. Cumulative energy and count have been widely used in fatigue damage evaluation during AE monitoring [6] [20] [25]. Therefore, these parameters have been chosen to compare the cumulative trend of AE entropy. It is evident in figure 7 that all three curves show the same trend. The initial rise in the cumulative parameters in region A, is due to the elastic to plastic transformation and mechanical noise. Region B is the damage accumulation stage and is accompanied by a very small increase in the cumulative parameters. A sudden rise in the cumulative parameters in regions C and E, is due to the growth and coalescence of micro cracks. Regions D and F are associated with a stable rise in the cumulative parameters. The stable rise in the cumulative parameters is associated with stable accumulation of micro damage such as micro crack growth. Region G is accompanied by a significant rise in the cumulative parameters. The sharp increase in the cumulative parameters in region G form 25,000 to 27,000s is due to macro fatigue crack initiation as suggested in [6] [7] [25] and the stable increase in the cumulative parameter from 27,000 to 29,500s is associated with stable macro fatigue crack

growth. The sharp increase in the cumulative parameters after 29,500s until the end is due to the result of rapid crack propagation, suggested in [6] [7] [25].

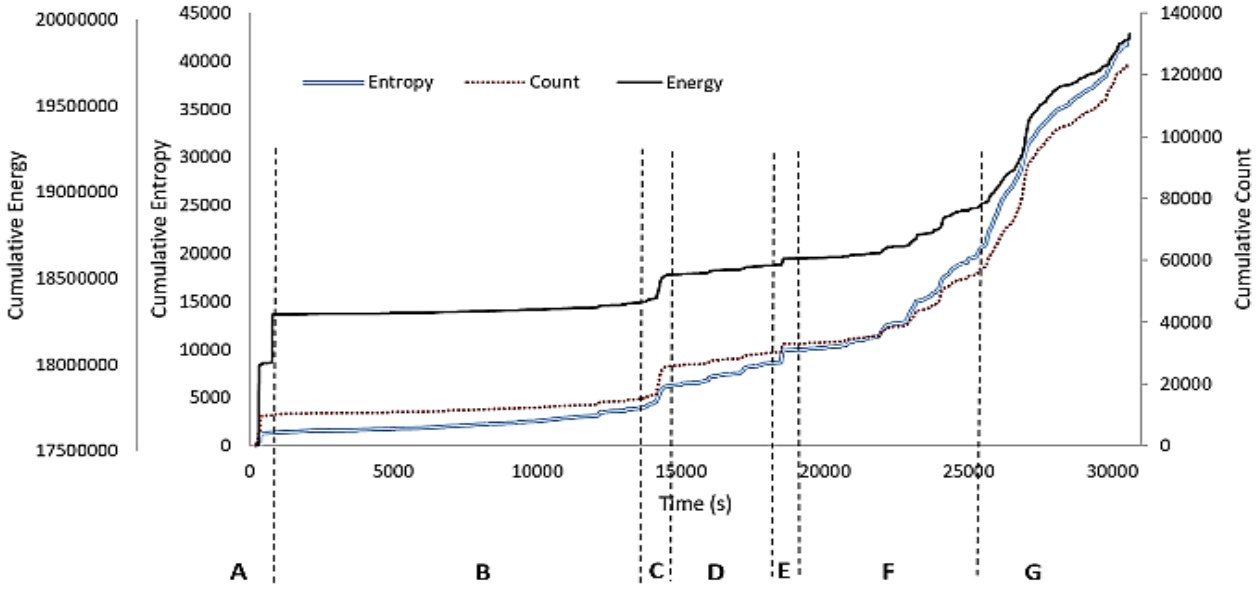

Fig 7: Cumulative entropy, cumulative energy and cumulative count versus time

The similar increasing trend in all three parameters showed that cumulative entropy can also be used as fatigue damage evaluation parameter instead of cumulative count and cumulative energy.

The above analysis indicates that AE entropy is sensitive to the fatigue damage evaluation in 316L stainless steel. The high peak amplitude distribution of the signal in the beginning of the test was associated with a lower value of AE entropy. Material damage, such as growth and coalescence of micro crack, macro fatigue crack initiation, propagation and ultimate failure was accompanied by a significant increase in AE entropy. Since AE entropy is a measure of uncertainty or randomness in a waveform, this suggest that waveform from material damage is associated with more uncertainty or randomness than that of noise. Moreover, cumulative entropy had a similar trend as the cumulative count and cumulative energy suggesting that the cumulative entropy can also be used as a fatigue damage evaluation parameter.

3.2. AE data collection with DIC

The secondary monitoring technique used in the first test was the %elongation of the material, which did not show any change in trend of fatigue damage evaluation except for the onset of loading and ultimate failure. To improve the performance of the secondary monitoring technique, the second test was conducted with Digital Image Correlation (DIC) measurement alongside AE monitoring.

DIC provided a full surface displacement and strain image over the entire gauge length of the specimen. There were several images taken during the test.

Figure 8 shows a few of the images captured by DIC during cyclic loading of the specimen. Image (a) in figure 8 is the reference image. This image was taken prior to loading of the specimen. Image (b) was taken at 11,188s after the start of the test. Image (c) was taken at 18,664s. It can be seen in image (c) that the macrostrain is localized in a small volume, marked by the black arrow. Localized macrostrain occurs long after the accumulation of micro crack initiation, coalescence and growth in the persistence slip band. In image (d) and (e) at 18,665s and 19,004s macro fatigue crack propagation can be identified from the localized macrostrain seen in (c). Image (f) at 19,400s shows the ultimate failure of the specimen captured by DIC.

DIC provides crucial information regarding fatigue damage evaluation. Firstly, information is obtained regarding macrostrain localization, because of micro fatigue crack initiation, coalescence and growth. Secondly, information is obtained regarding macro fatigue crack propagation leading to the ultimate failure of the specimen.

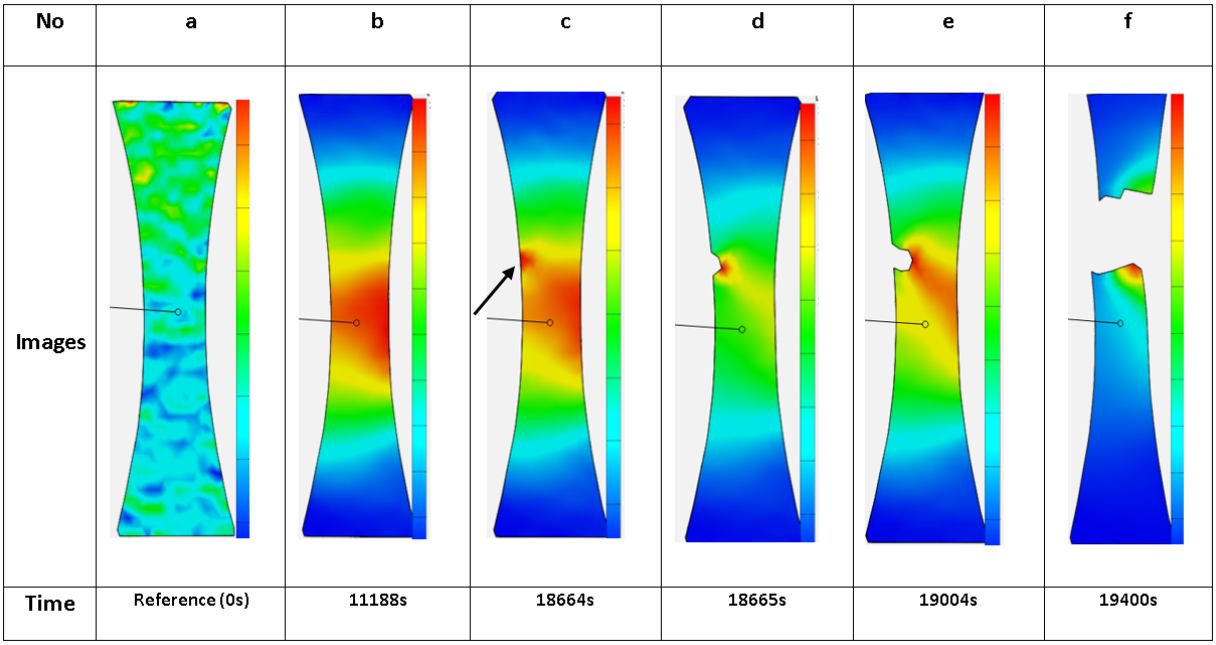

Fig 8: Digital Image Correlation images

Figure 9 shows a plot of cumulative count, cumulative energy and cumulative entropy for the entire length of the second test. Like the first test, it is clear from the graph that all curves have the same trend. A significant increase in the cumulative parameters in region A, can be attributed to the elastic to plastic transformation and mechanical noise originating from the metal to metal contact at the specimen grips. The damage accumulation stage in region B is accompanied by a minimum increase in the cumulative parameters. A sharp increase in the cumulative parameters in region C and E can be associated with micro crack coalescence and growth, whereas a stable increase in the cumulative parameters in region D and F is due to a stable accumulation of micro crack growth in the material. After the onset of macrostrain localization, macro fatigue crack initiates, which is accompanied by a sharp increase in the cumulative parameters. This trend is also consistent with other research [6] [7]. After macro fatigue crack initiation, the cumulative parameters show a stable variation between 18,700s to 19,300s. This region is associated with stable macro crack propagation. The stable increase in cumulative parameters due to stable macro fatigue crack propagation is also consistent with other researchers [6] [7] [21]. The sharp increase in the cumulative parameter at the end, after 19,300s, is due to an unstable crack propagation, suggested by [6] [7] [21].

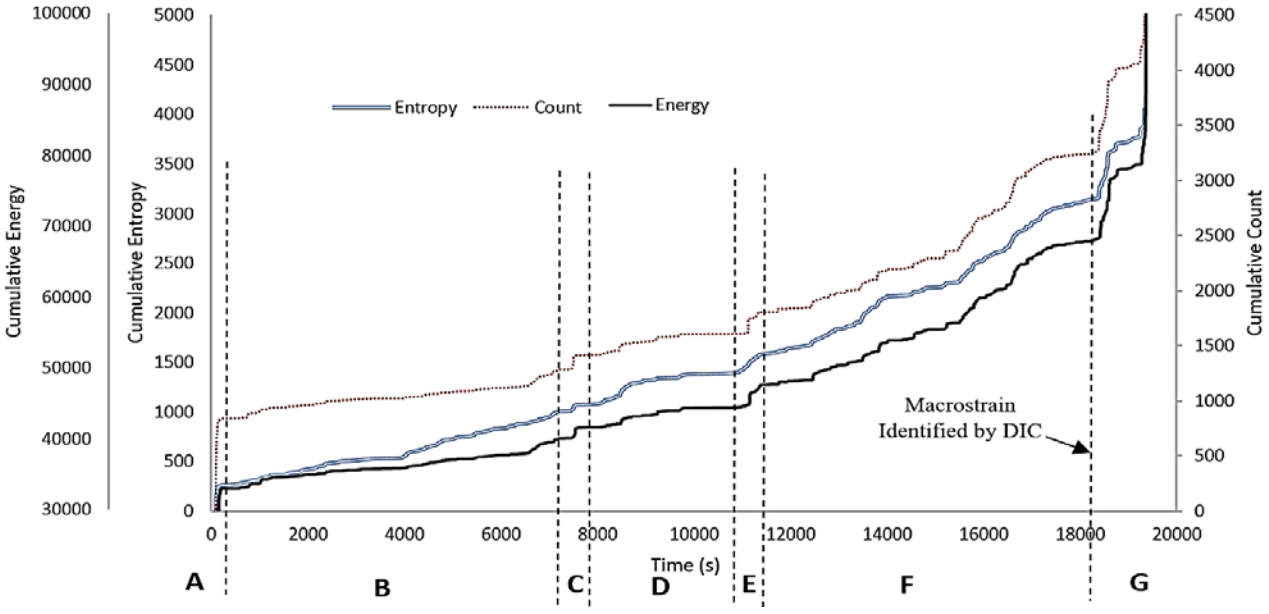

Fig 9: Cumulative entropy, cumulative energy and cumulative count versus time

4. Conclusion

In this paper, a new qualitative parameter called AE entropy, based on Renyi's entropy has been proposed. The new parameter proved effective in discriminating different stage of damage during a fatigue endurance test, leading to ultimate failure of 316L stainless steel. AE entropy is a measure of uncertainty of the amplitude distribution of the waveform. Therefore it is independent of time driven parameters and threshold. The following can be concluded form the results obtained during these experiments:

- A comparison between AE entropy and traditional AE peak amplitude measurements concluded that the initial increase in the peak amplitude of the signal as a result of elastic to plastic transformation and mechanical noise, is associated with a lower value of AE entropy. Growth and coalescence of micro crack, macro crack initiation, macro crack propagation and ultimate failure is associated with a higher entropy value. This could provide an effective method for characterizing damage in the material.

- Cumulative AE entropy, cumulative count and cumulative energy followed the same trend during the fatigue endurance test of 316L stainless steel. The traditional AE cumulative analysis during fatigue based on count and energy, can be replaced with AE entropy, because of its independent nature in terms of time driven parameter and threshold.

Acknowledgements: - This publication was made possible by the sponsorship and support of London South Bank University and Lloyd's Register Foundation, a charitable foundation helping protect life and property by supporting engineering-related education, public engagement, and the application of research. The work was enabled through, and undertaken at, the National Structural Integrity Research Centre (NSIRC), a postgraduate engineering facility for industry-led research into structural integrity established and managed by TWI through a network of both national and international Universities.

References

1. C.J.Hailer, *Handbook of Nondestructive Evaluation-Chapter 10*,(The McGraw-Hill Companies, 2001).
2. M. David, R.B.K.N. Rao, Shock and Vibration Digest, **38**, 3-16, (2006).
3. C. Boller, *Sixth European Workshop on Structural Health Monitoring*, (Dresden 2012).
4. A.C.E. Sinclair, D.C. Connors,C.L. Formby, Material Science and Engineering, **28**, 263-273, (1977).
5. R. Roy, N. Parida, S.Sivaprasad, S. Tarafder. K.K.Ray, Meterial Science and Engineering A, **486**, 562-571, (2008).
6. Z. Han, H. Lou, J. Cao and H. Wang, Materials Science and Engineering A, **528**, 7751– 7756, (2011).
7. Z. Han, H. Luo, Y. Zhang and J. Cao, Materials Science & Engineering A, **559**, 534-542, (2012).
8. H. Zhiyuan, L. Hongyun, S. Chuankai, L. Junrong and P. Mayorkinos, Material Science & Engineering A, **597**, 270-278, (2014).
9. D.G.Aggelis, E.Z.Kordatos and T.E.Matikas, Machenics Research Communication, **38**, 106-110, (2011).
10. T.M.Roberts, M.Talebzadeh , Journal of construction steel reserach, **59**, 679-694, (2003).
11. C. Mengyu, Z. Zhang, D. Quan and Y. Song, International Journal of Fatigue, **109**, 145-156, (2018).
12. C. Mengyu, Z. Zaoxiao and D. Quan, Mechanical sytems and signal processing, **100**, 617-629, (2018).
13. A. Renyi, Proc. of the 4th Berkeley Symp. Math. Statist. Prob, **1**, 457-561, (1960).
14. D. Xu and E. Deniz, *Information Theoretic Learning* (47-102, New York, NY: Springer, 2010).
15. Gray. M, Robert. *Entropy and Information Theory*, (Boston, MA: Springer, 2011).
16. K. Ekˇstein, T. Pavelka, In *Proceedings of PhD Workshop Systems & Control,* University of West Bohemia, (2004).
17. A.Vahaplar,C.C.Celikoglu,M.Ozgoren,Mathematical and Computational Applications, **16**,43-52, (2011).
18. V. Vijean, M. Hariharan, S. Yaacob, M. Nazri, B. Sulaiman and A. Adom, Computers and Electrical Engineering, **39**,1549–1560, (2013).
19. V.Vijean, H.M, S, Yaacob, M.N.B.Sulaiman, Biocybernetics and Biomedical Engineering, **34**,169-177, 2014.
20. O. A. Amer, A.-L. Gloanec, S. Courtin, C. Touze, *Procedia Engineering*,**66**,651-660, (2013).
21. K.S.Han,K.H.Oh, Key Engineering Materials,**306-308**, 271-278, (2006).
22. M. Chai, Z. Zhang, Q. Duan and Y. Song, International Journal of Fatigue, **109**, 145-156, (2018).
23. D. Barktova, F. Vlasic, P. Mazal and O. Dvoracek, *In Metal 23rd International Conference on Metallurgy and Materials,* 1-6 (2014).
24. P. Mazal, F. Vlasic and V. Koula, *Procedia Engineering*, **133**, 379-388,(2015).
25. M.Chai,J.Zhang, Z.Zhang, Q.Duan, G.Cheng. Applied Acoustics,**126**,101-113, (2017).